Journal of Applied Physics

Photoemission characteristics of thin GaAs-based heterojunction photocathodes

Cheng Feng, Yijun Zhang, Yunsheng Qian, Feng Shi, Jijun Zou, and Yugang Zeng

Citation: Journal of Applied Physics **117**, 023103 (2015); doi: 10.1063/1.4905621
View online: http://dx.doi.org/10.1063/1.4905621
View Table of Contents: http://scitation.aip.org/content/aip/journal/jap/117/2?ver=pdfcov
Published by the AIP Publishing

Photoemission characteristics of thin GaAs-based heterojunction photocathodes

Cheng Feng,[1] Yijun Zhang,[1,a)] Yunsheng Qian,[1] Feng Shi,[2] Jijun Zou,[3] and Yugang Zeng[4]
[1]*Institute of Electronic Engineering and Optoelectronic Technology, Nanjing University of Science and Technology, Nanjing 210094, China*
[2]*Science and Technology on Low-Light-Level Night Vision Laboratory, Xi'an 710065, China*
[3]*Engineering Research Center of Nuclear Technology Application (East China Institute of Technology), Ministry of Education, Nanchang 330013, China*
[4]*Changchun Institute of Optics, Fine Mechanics and Physics, Chinese Academy of Sciences, Changchun 130033, China*

(Received 13 November 2014; accepted 26 December 2014; published online 8 January 2015)

To better understand the different photoemission mechanism of thin heterojunction photocathodes, the quantum efficiency models of reflection-mode and transmission-mode GaAs-based heterojunction photocathodes are revised based on one-dimensional continuity equations, wherein photoelectrons generated from both the emission layer and buffer layer are taken into account. By comparison of simulated results between the revised and conventional models, it is found that the electron contribution from the buffer layer to shortwave quantum efficiency is closely related to some factors, such as the thicknesses of emission layer and buffer layer and the interface recombination velocity. Besides, the experimental quantum efficiency data of reflection-mode and transmission-mode AlGaAs/GaAs photocathodes are well fitted to the revised models, which confirm the applicability of the revised quantum efficiency models.
[http://dx.doi.org/10.1063/1.4905621]

I. INTRODUCTION

With the advantages of high quantum efficiency, low dark current, good long-wavelength response and narrow energy spread, GaAs photocathodes and ternaries based on them, have shown substantially improved performance and widespread application in the weak light detection and high energy physics.[1–4] Recently, a novel concept of photon-enhanced thermionic emission based on GaAs-based heterojunction photocathode was proposed to boost conversion efficiency of photovoltaic cells.[5] As for various GaAs-based photocathodes in practice, the quantum efficiency is distinctly a very important parameter utilized to evaluate the performance of photocathodes. Achieving high quantum efficiency, large polarization and good stability for thin GaAs-based photocathodes is an important topic for quite a long time in the research of favorable electron source.[6–8] As the proposed three-step model known as the bulk effect, the photoemission is treated in terms of photoexcitation, electron transport to the surface, and escape to vacuum.[9] This three-step model theory provides a means of detailed understanding practical photoemission and theoretical guidance to design high-performance photocathodes. Accordingly, the conventional quantum efficiency models were derived by solving the one-dimensional continuity equations based on the three-step model.[10–12]

With the development of material growth techniques and the goal of improving the quantum efficiency of photocathodes, a series of GaAs-based heterojunction structures with different thin buffer layers and emission layers were realized.[13–15] In many practical applications, a buffer layer is used to match with the lattice of emission layer and prevent photoelectron contributions from the substrate.[16] On the other hand, when the epitaxial emission layer is thin enough, the buffer layer should also participate in photoemission of the heterojunction photocathodes and improve the quantum efficiency as well. Nevertheless, the available quantum efficiency models cannot afford effective approaches to well fit the experimental quantum efficiency curves, which exhibit the shape like the "dual-knee-bend" rather than "single-knee-bend."[17–19]

Since the lack of proper quantum efficiency models for evaluating thin GaAs-based photocathodes, how the buffer layer in the multilayer structure acts on quantum efficiency is not clear, and the mechanism of photoemission from these thin heterojunction photocathodes is still not well understood. In this paper, we revise the quantum efficiency models for typical reflection-mode (r-mode) and transmission-mode (t-mode) AlGaAs/GaAs heterojunction photocathodes by solving from the one-dimensional continuity equations according to three-step model theory. In the revised quantum efficiency models, the photoelectron contributions from the buffer layer and the additional factors such as the thickness of buffer layer and interface recombination velocity for both r-mode and t-mode photocathodes are all taken into account. According to the revised model, we analyze some related cathode performance parameters which have great effect on the characteristics of quantum efficiency values in combination with the conventional model, including thicknesses of the emission layer and the buffer layer, and the interface recombination velocity. Finally, in order to verify the theoretical practicality, two types of thin AlGaAs/GaAs

a)E-mail: zhangyijun423@126.com

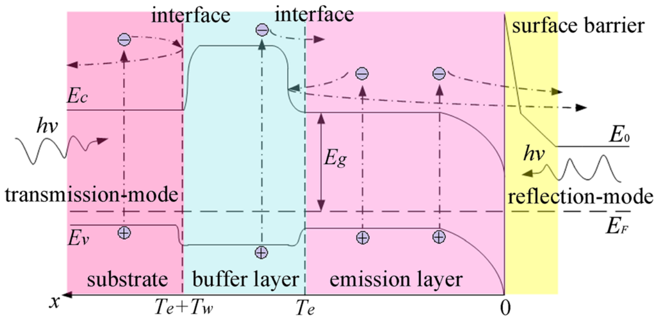

FIG. 1. Energy band structure diagram of the GaAs-based heterojunction photocathode. E_c is the conduction-band minimum, E_v is the valence band maximum, E_g is the bandgap, E_F is the Fermi level, E_0 is the vacuum level.

photocathodes operating in r-mode and t-mode are prepared, respectively, to investigate the spectral characteristics, and cathode performance parameters are analyzed through accurate curve fitting with aid of the revised quantum efficiency models.

II. THEORETICAL REVISION

The energy band structure of the GaAs-based heterojunction photocathode is shown in Fig. 1. The main difference between r-mode and t-mode photocathodes depends on the direction of incident light. For r-mode photocathode, when the incident light illuminates onto the photocathode, the emission layer absorbs a majority of high-energy photons and generates photoexcited electrons in the bulk. The photoelectrons from the bulk transport to the surface by diffusion traverse across the potential barrier and finally escape to vacuum. Meanwhile, some excited electrons generated nearby the back interface of emission and buffer layer are recombined at the interface, and others will transport into the emission layer rather than diffuse into the buffer layer due to the potential barrier at the interface. As the polarization is inversely proportional to the thickness of emission layer, the emission layer is usually designed to be thin enough. For this case, there is reason to believe that the high-energy photons can be absorbed by the buffer layer as well. The buffer layer generates photoelectrons, and the photoelectrons diffuse into emission layer and at last escape to vacuum. Some photons probably are absorbed in substrate, but the photoexcited electrons cannot diffuse into buffer layer to contribute to the spectral response because of the existence of potential barrier between the substrate and buffer layer. For t-mode photocathode, when the incident light illuminates onto the substrate, most photons will penetrate into the buffer layer. The buffer layer can absorb high-energy photons and generate photoelectrons. If the buffer layer is thin, parts of the photoelectrons will diffuse into the emission layer, and finally escape to vacuum. For the same reason, some long-wave photons passing through the buffer layer can be absorbed by the emission layer and generate photoelectrons as well.

Based on the three-step model theory of photoemission, the electrons escape from the bulk to produce photoemission mainly by diffusion. For uniform-doped r-mode and t-mode GaAs-based heterojunction photocathodes, the transport of photoexcited electrons in the emission layer follows the one-dimensional continuity equations, which are, respectively, given by

$$D_n \frac{d^2 n_1(x)}{dx^2} - \frac{n_1(x)}{\tau_1} + (1 - R_{hv}) I_0 \alpha_{hv} \times \exp(-\alpha_{hv} x) = 0,\ x \in [0, T_e] \tag{1}$$

$$D_n \frac{d^2 n_1(x)}{dx^2} - \frac{n_1(x)}{\tau_1} + (1 - R_{hv}) I_0 \alpha_{hv} \exp(-\beta_{hv} T_w) \times \exp[-\alpha_{hv}(T_e - x)] = 0,\ x \in [0, T_e], \tag{2}$$

where $n_1(x)$ is the concentration of minority carrier (i.e., electrons) in emission layer, τ_1 is the lifetime of electrons in emission layer, D_n is the diffusion coefficient of electrons, μ is electron mobility, I_0 is the intensity of incident light, α_{hv} is the absorption coefficient of the material in emission layer, R_{hv} is the reflectivity on the surface of photocathode, β_{hv} is the absorption coefficient of buffer layer, and T_e and T_w are the thickness of the emission layer and the buffer layer, respectively.

When defining the boundary conditions as the solution to Eqs. (1) and (2), one of them should take account of the electron contributions from the buffer layer. Accordingly, the boundary conditions suitable for the thin GaAs-based heterojunction photocathodes are given by

$$n_1(x)|_{x=0} = 0 \tag{3}$$

$$D_n \frac{dn_1(x)}{dx}\bigg|_{x=T_e} = -S_V n_1(x)|_{x=T_e} + S_V n_{buf}, \tag{4}$$

where S_v is the back interface recombination velocity, n_{buf} represents the number of electrons that generate at the back interface of the buffer layer.

Upon applying the boundary conditions to Eqs. (1) and (2), we can obtain the concentration of electrons $n_1(x)$ in the emission layer. After $n_1(x)$ is substituted into $Y(hv) = PD_n \frac{dn_1(x)}{dx}|_{x=0}/I_0$, the revised quantum efficiency formulae for uniform-doped r-mode and t-mode are derived as follows:

$$Y_R(hv) = \frac{PD_n S_V n_{buf}}{I_0[D_n \cosh(T_e/L_D) + S_v L_D \sinh(T_e/L_D)]} + \frac{P(1 - R_{hv})\alpha_{hv} L_D}{\alpha_{hv}^2 L_D^2 - 1} \times \left\{ \frac{L_D(S_v - \alpha_{hv} D_n)\exp(-\alpha_{hv} T_e) - S_v L_D \cosh(T_e/L_D) - D_n \sinh(T_e/L_D)}{[D_n \cosh(T_e/L_D) + S_v L_D \sinh(T_e/L_D)]} + \alpha_{hv} L_D \right\} \tag{5}$$

$$Y_T(h\nu) = \frac{PD_nS_vn_{buf}}{I_0[D_n\cosh(T_e/L_D) + S_vL_D\sinh(T_e/L_D)]} + \frac{P(1-R_{h\nu})\alpha_{h\nu}L_D\exp(-\beta_{h\nu}T_w)}{\alpha_{h\nu}^2L_D^2-1} \times \left[\frac{L_D(S+\alpha_{h\nu}D_n) - [S_vL_D\cosh(T_e/L_D) + D_n\sinh(T_e/L_D)]\exp(-\alpha_{h\nu}T_w)}{D_n\cosh(T_e/L_D) + S_vL_D\sinh(T_e/L_D)} - \alpha_{h\nu}L_D\exp(-\alpha_{h\nu}T_e)\right], \tag{6}$$

where P is the surface electron escape probability, L_D is the diffusion length of the minority carrier (i.e., electrons) in the emission layer. In order to obtain n_{buf}, the one-dimensional continuity equations which stand for the transport of photo-excited electrons in the buffer layer of r-mode and t-mode GaAs-based heterojunction photocathodes should be solved as follows:

$$D_n\frac{d^2n_2(x)}{dx^2} - \frac{n_2(x)}{\tau_2} + (1-R_{h\nu})I_0\beta_{h\nu}\exp(-\alpha_{h\nu}T_e) \times \exp[-\beta_{h\nu}(x-T_e)] = 0,\ x\in[T_e, T_e+T_w] \tag{7}$$

$$D_n\frac{d^2n_2(x)}{dx^2} - \frac{n_2(x)}{\tau_2} + (1-R_{h\nu})I_0\beta_{h\nu} \times \exp[-\beta_{h\nu}(T_e+T_w-x)] = 0,\ x\in[T_e, T_e+T_w]. \tag{8}$$

For solving Eqs. (7) and (8), the boundary conditions are given by

$$D_n\frac{dn_2(x)}{dx}\Big|_{x=T_e} = S_Vn_2(x)|_{x=T_e} \tag{9}$$

$$n_2(x)|_{x=T_e+T_w} = 0. \tag{10}$$

Through solving Eqs. (7) and (8) combined with Eqs. (9) and (10), we can obtain the electron concentration at the back interface of the buffer layer. Following that, the obtained values of n_{buf} are substituted into Eqs. (5) and (6), respectively, the final quantum efficiency formulae for thin r-mode and t-mode heterojunction photocathodes are given by

$$Y_R(h\nu) = \frac{PS_V(1-R_{h\nu})\beta_{h\nu}\exp(-\alpha_{h\nu}T_e)\exp(-\beta_{h\nu}T_e)L_n^2}{\left(1-\beta_{h\nu}^2L_n^2\right)[D_n\cosh(T_e/L_D)+S_vL_D\sinh(T_e/L_D)]} \times \left[\frac{(D_n/L_D)\cosh(T_w/L_n) - D_n\beta_{h\nu}\sinh(T_w/L_n) - (D_n/L_n)\exp(-\beta_{h\nu}T_w)}{(D_n/L_n)\cosh(T_w/L_n) + S_v\sinh(T_w/L_n)}\right] + \frac{P(1-R_{h\nu})\alpha_{h\nu}L_D}{\alpha_{h\nu}^2L_D^2-1} \times \left\{\frac{L_D(S_v-\alpha_{h\nu}D_n)\exp(-\alpha_{h\nu}T_e) - S_vL_D\cosh(T_e/L_D) - D_n\sinh(T_e/L_D)}{[D_n\cosh(T_e/L_D)+S_vL_D\sinh(T_e/L_D)]} + \alpha_{h\nu}L_D\right\} \tag{11}$$

$$Y_T(h\nu) = \frac{PD_nS_v\beta_{h\nu}(1-R_{h\nu})\left(L_n^2/D_n\right)}{\left(1-\beta_{h\nu}^2L_n^2\right)[D_n\cosh(T_e/L_D)+S_vL_D\sinh(T_e/L_D)]} \times \left[\frac{(D_n\beta_{h\nu}-S_V)\exp(-\beta_{h\nu}T_w)\sinh(T_w/L_n) - (D_n/L_n)}{(D_n/L_n)\cosh(T_w/L_n) + S_V\sinh(T_w/L_n)} + \exp(-\beta_{h\nu}T_w)\right] + \frac{P(1-R_{h\nu})\alpha_{h\nu}L_D\exp(-\beta_{h\nu}T_w)}{\alpha_{h\nu}^2L_D^2-1} \times \left[\frac{L_D(S+\alpha_{h\nu}D_n) - [S_vL_D\cosh(T_e/L_D)+D_n\sinh(T_e/L_D)]\exp(-\alpha_{h\nu}T_w)}{D_n\cosh(T_e/L_D)+S_vL_D\sinh(T_e/L_D)} - \alpha_{h\nu}L_D\exp(-\alpha_{h\nu}T_e)\right], \tag{12}$$

where $L_n = (D_n\tau_2)^{1/2}$, and L_n is the diffusion length of the minority carrier (i.e., electrons) in the buffer layer.

III. THEORETICAL SIMULATION

In order to figure out the impact of photoelectrons generated in the buffer layer on spectral characteristics of GaAs-based heterojunction photocathodes, we analyze the factors including the thicknesses of emission layer and buffer layer, and the interface recombination velocity acting on the quantum efficiency utilizing Eqs. (11) and (12). In order to highlight the differences of the revised quantum efficiency models, the conventional models excluding electron contribution from the buffer layer are simulated meanwhile, and the formulae are given by

$$Y_R'(h\nu) = \frac{P(1-R_{h\nu})\alpha_{h\nu}L_D}{\alpha_{h\nu}^2L_D^2-1} \times \left[\frac{L_D(S_v-\alpha_{h\nu}D_n)\exp(-\alpha_{h\nu}T_e) - S_vL_D\cosh(T_e/L_D) - D_n\sinh(T_e/L_D)}{D_n\cosh(T_e/L_D)+S_vL_D\sinh(T_e/L_D)} + \alpha_{h\nu}L_D\right] \tag{13}$$

$$Y'_T(h\nu) = \frac{P(1-R_{h\nu})\alpha_{h\nu}L_D\exp(-\beta_{h\nu}T_w)}{\alpha_{h\nu}^2 L_D^2 - 1} \times \left[\frac{L_D(S+\alpha_{h\nu}D_n) - [S_v L_D\cosh(T_e/L_D) + D_n\sinh(T_e/L_D)]\exp(-\alpha_{h\nu}T_w)}{D_n\cosh(T_e/L_D) + S_v L_D\sinh(T_e/L_D)} - \alpha_{h\nu}L_D\exp(-\alpha_{h\nu}T_e)\right]. \quad (14)$$

In the simulation, we choose $Al_{0.7}Ga_{0.3}As$/GaAs heterojunction photocathode as an example and some parameters are fixed, wherein $P = 0.5$, $D_n = 120\,\mathrm{cm^2/s}$, $L_D = 3\,\mu\mathrm{m}$, $L_n = 0.8\,\mu\mathrm{m}$, $R_{h\nu} = 0.31$[10], $\alpha_{h\nu}$ and $\beta_{h\nu}$ are referred to Refs. 20 and 21.

We first investigate the effect of the thickness of GaAs emission layer T_e on quantum efficiency, and the changes of theoretical quantum efficiency curves with various thicknesses of the emission layer are shown in Fig. 2. The solid lines and dashed lines correspond to the simulated quantum efficiency curves using the revised model and conventional model, respectively. As shown in Fig. 2(a) assuming $S_v = 10^7\,\mathrm{cm/s}$ and $T_w = 0.5\ \mu\mathrm{m}$, the quantum efficiency of r-mode photocathode in the entire waveband region is enhanced with the increase in T_e, which would provide ample space to absorb photons and generate more electrons. Until the complete light absorption in the bulk, the quantum efficiency curve will be unchanged even if T_e continues to increases. Besides, it is noted that the quantum efficiency denoted by the solid line in the high-energy region is always higher than that denoted by the dotted line, until T_e reach 0.1 μm. After that, the solid line and dashed line will have almost no difference. The simulated results show that when the GaAs emission layer is thin enough, photoelectrons generated in the AlGaAs buffer layer have obvious impact on the quantum efficiency of r-mode photocathodes. Because the band gap of this buffer layer is large, only shortwave photons with high energy can be absorbed. Therefore, the quantum efficiency in the shortwave region is mainly influenced as T_e decreases, because more shortwave photons passing through the emission layer will be absorbed by the buffer layer and more photoelectrons will be generated to increase the final quantum efficiency of the photocathode. When the emission layer is thick enough, the high-energy and low-energy photons are absorbed completely by the emission layer, and no shortwave photons could be absorbed by the buffer layer, which causes the coincidence of the solid and dashed lines. As for the t-mode photocathode, the thickness of the GaAs emission layer is usually controlled within 2 μm in practical applications.[22] As shown in Fig. 2(b) assuming $S_v = 10^6\,\mathrm{cm/s}$ and $T_w = 0.5\ \mu\mathrm{m}$, the diversification of quantum efficiency depends on the various thicknesses of GaAs emission layer. The longwave response induced in the GaAs layer is improved with the increase in T_e. The photoexcited electrons in the buffer layer mainly influence the quantum efficiency in the shortwave region, and there is almost no significant change of curves when the thickness of the GaAs emission layer varies in the range of 2 μm. It indicates that for the t-mode photocathode with backside illumination, the photoexcited electrons in the AlGaAs layer can transport to the GaAs emission layer and finally escape to the vacuum under suitable preconditions.

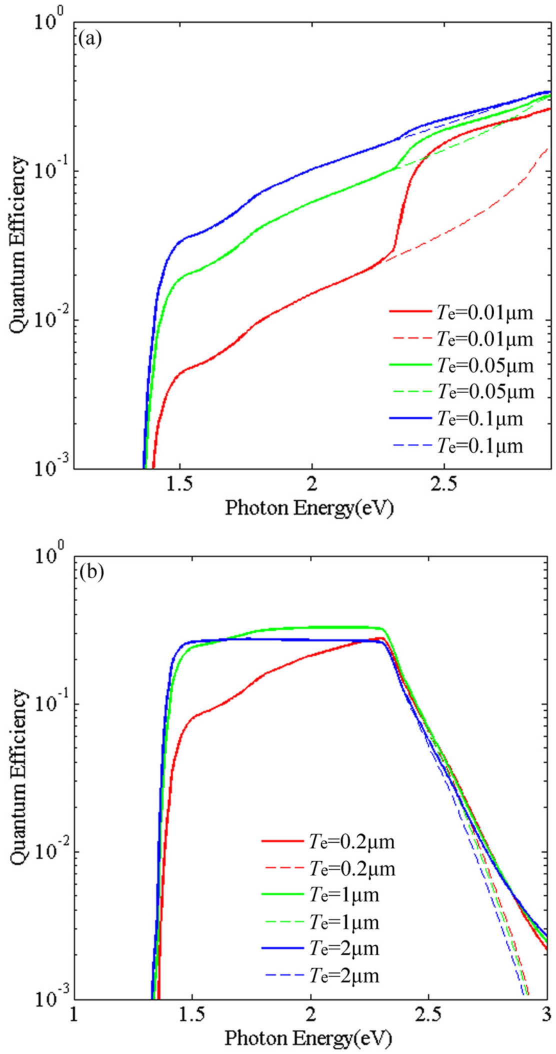

FIG. 2. Theoretical quantum efficiency curves with the change of T_e for AlGaAs/GaAs photocathodes operating in the (a) r-mode and (b) t-mode, respectively.

Fig. 3 shows the theoretical quantum efficiency curves with various thicknesses of the buffer layer. The solid lines and dashed lines correspond to the simulated quantum efficiency curves using the revised model and conventional model, respectively. For the r-mode photocathode, as mentioned above, when the emission layer is thin enough, it could not absorb shortwave photons adequately, and thus parts of shortwave photons are absorbed by the buffer layer. It is clear to see that the thickness of buffer layer T_w also influences the final quantum efficiency values in the shortwave region. In Fig. 3(a) assuming $S_v = 10^7\,\mathrm{cm/s}$ and $T_e = 0.01\ \mu\mathrm{m}$, the dashed lines coincide with each other because Eq. (13) excludes the factor of AlGaAs buffer layer. In fact, the AlGaAs buffer layer can absorb more shortwave light and generate more electrons as T_w increases under the condition that the emission layer is thin enough. The difference between the solid line and dashed

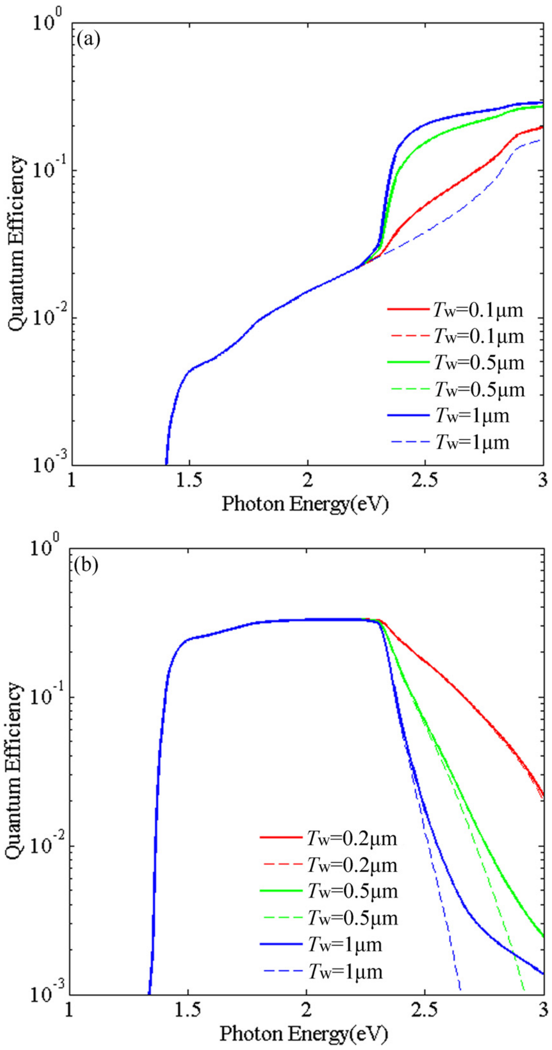

FIG. 3. Theoretical quantum efficiency curves with the change of T_w for AlGaAs/GaAs photocathodes operating in the (a) r-mode and (b) t-mode, respectively.

line becomes more obvious as T_w increases until T_w reaches 1 μm, which represents the maximum shortwave absorption length in the buffer layer. We can find that the AlGaAs buffer layer not only plays a role in matching lattice with GaAs emission layer, but also makes a significant contribution to enhance the quantum efficiency to a certain extent. For t-mode photocathode, the thickness of the AlGaAs layer also designs to be thin in practical application to improve the quantum efficiency in the shortwave region of the photocathode.[23] As a result of the large absorption coefficient of shortwave light in GaAlAs, the thickness of buffer layer is usually no more than 1 μm in practical applications.[22] As shown in Fig. 3(b) assuming $S_v = 10^6$ cm/s and $T_e = 1$ μm, the quantum efficiency in the shortwave region decreases as T_w increases because of the shortwave constraint factor in Eqs. (12) and (14).[24] When T_w is thin, less shortwave light is absorbed in the AlGaAs buffer layer, instead, most of the shortwave light penetrating through the AlGaAs layer is absorbed by the GaAs emission layer and generate electrons. Therefore, the solid line coincides with the dashed line in the case of slightly thin buffer layer. Compared with the AlGaAs buffer layer, the GaAs emission layer with superior electron emission efficiency has more contributions to the quantum efficiency in the shortwave region. On the other hand, the AlGaAs buffer layer is usually thought to serve as the shortwave filter for photocathode operating in the t-mode, whereas, as T_w increases, more electrons can generate in the buffer layer and diffuse into the emission layer if the back interface recombination is not so serious. In this case, considering the influence of the buffer layer on quantum efficiency in the shortwave region is necessary.

As another key characteristic parameter, the back interface recombination velocity between the emission layer and buffer layer also plays an important role in the electron contribution of buffer layer to the final quantum efficiency. The simulated results are shown in Fig. 4, wherein the solid lines and dashed lines correspond to the simulated quantum efficiency curves using the revised model and conventional model, respectively. For the r-mode photocathode, as shown in Fig. 4(a) assuming $T_e = 0.01$ μm and $T_w = 0.5$ μm, it is found that the photoexcited electrons in the buffer layer can improve the quantum efficiency only when S_v is in the range of 10^6–10^9 cm/s. Quantum efficiency curves corresponding to revised model and conventional model substantially coincide in the case of either

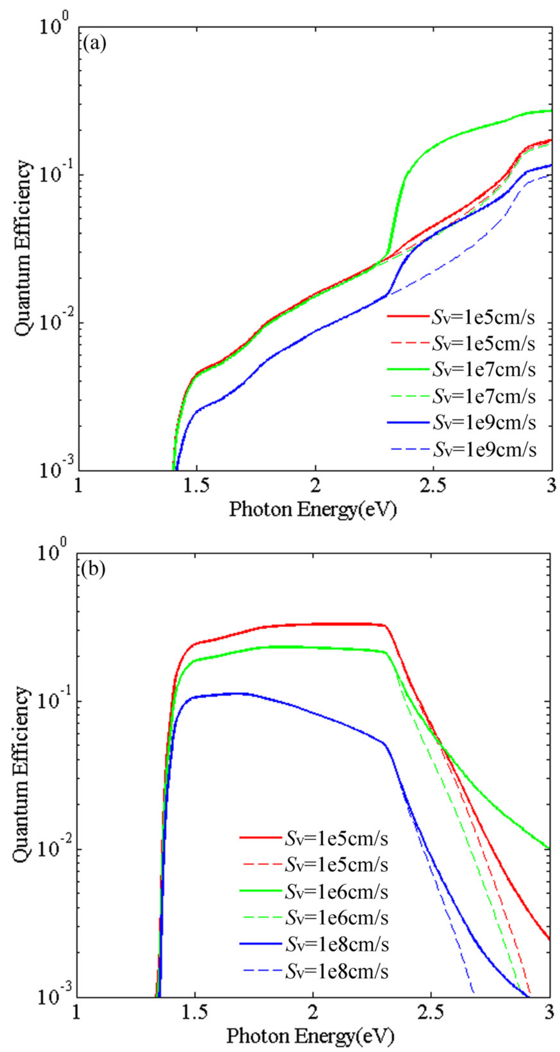

FIG. 4. Theoretical quantum efficiency curves with the change of S_v for AlGaAs/GaAs photocathodes operating in the (a) r-mode and (b) t-mode, respectively.

$S_v \leq 10^5$ cm/s or $S_v \geq 10^{10}$ cm/s. When $S_v \leq 10^5$ cm/s, most photoelectrons originating from the buffer layer will diffuse to the substrate and finally recombine and disappear because of the larger recombination velocity between the buffer layer and substrate. When $S_v \geq 10^{10}$ cm/s, the photoelectrons will transport to the back interface to make up a loss of recombined electrons nearby the AlGaAs/GaAs back interface. If the interface recombination velocity is too large, all complementary electrons from the buffer layer will be recombined instead of diffusing into the emission layer. In addition, it is noted that the large back interface recombination velocity is extremely adverse to the quantum efficiency in the entire waveband region. Naturally, the buffer layer has almost no impact on the final quantum efficiency of the photocathodes as well. As for the t-mode quantum efficiency curves in Fig. 4(b), wherein $T_e = 1\ \mu$m and $T_w = 0.5\ \mu$m, it is also found that there is no difference between quantum efficiency curves corresponding to the revised model and conventional model when $S_v \leq 10^4$ cm/s. Like the case of r-mode photocathode, because of the larger interface recombination velocity between the buffer layer and substrate, most electrons generated in the AlGaAs layer will diffuse to the substrate to compensate rather than transport to the AlGaAs/GaAs back interface. When $S_v \geq 10^5$ cm/s, the photoexcited electrons in the AlGaAs layer can contribute to the quantum efficiency and more and more electrons are able to transport to the back interface and make the shortwave quantum efficiency increase. If the recombination velocity exceeds 10^9 cm/s or even larger, the electrons transporting to the back interface are nearly recombined and quantum efficiency curves corresponding to revised model and conventional model will coincide again. From the simulated results, it can be inferred that only when the back interface recombination velocity is appropriate, the electrons generated from the buffer layer can act on the quantum efficiency in the shortwave region for r-mode and t-mode photocathodes.

IV. EXPERIMENT AND ANALYSIS

To verify the practicality of the revised quantum efficiency models for r-mode and t-mode GaAs-based heterojunction photocathodes, two types of AlGaAs/GaAs heterojunction photocathodes operating in the r-mode and t-mode were prepared, respectively. The two AlGaAs/GaAs heterojunction epilayers were grown on the high quality n-type GaAs (100)-oriented substrates by the metal-organic chemical vapor deposition (MOCVD) technique. The p-type zinc doping concentration for both the AlGaAs buffer layer and GaAs emission layer is 1×10^{19} cm^{-3}. Different epilayer structures were grown, wherein the Al mole fraction in the buffer layer is 0.6 and 0.7 for the r-mode and t-mode samples, respectively. The thicknesses of AlGaAs buffer layer and GaAs emission layer for r-mode sample are 1 μm and 0.02 μm, while those for t-mode sample are 0.4 μm and 1.3 μm. During the growth procedure, the V/III ratio was kept at 10–15, and the growth temperature was 710 °C for AlGaAs and 680 °C for GaAs.

Differing from the r-mode sample, the as-grown t-mode sample was made into the cathode module with a glass/Si_3N_4/AlGaAs/GaAs structure by bonding and selective etching, as the proposed process of fabricating t-mode GaAs photocathodes by Antypas *et al.*[25] Prior to activation, the samples underwent a two-step surface preparation consisting of a wet chemical cleaning process and a heat treatment process in vacuum to eliminate the surface contamination, such as oxides and carbon. The negative-electron-affinity (NEA) activation for the two photocathodes was performed in an ultrahigh vacuum chamber with base pressure less than 10^{-8} Pa by using the cesium and oxygen co-deposition technique.[26,27] After the usual "high-low temperature" two-step activation,[28] the quantum efficiency curve of the r-mode photocathode was measured *in situ* by the on-line quantum efficiency measurement system, while that of the t-mode photocathode sealed in the image tube was measured after transferred into ambient air.[29]

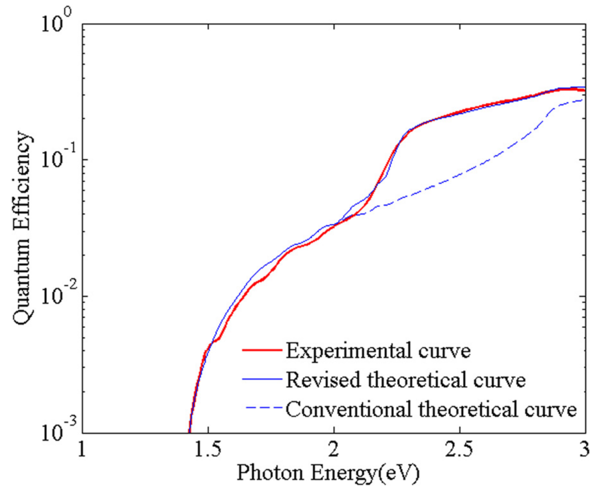

FIG. 5. Experimental quantum efficiency curve of the r-mode $Al_{0.6}Ga_{0.4}As$/GaAs photocathode and the fitted curves via the revised model and the conventional model, respectively.

The experimental quantum efficiency curves denoted by red solid line are shown in Figs. 5 and 6 for the r-mode and t-mode AlGaAs/GaAs samples, respectively. The quantum efficiency curve for the r-mode sample exhibits the shape like "dual-knee-bend" arising from the thin emission layer.

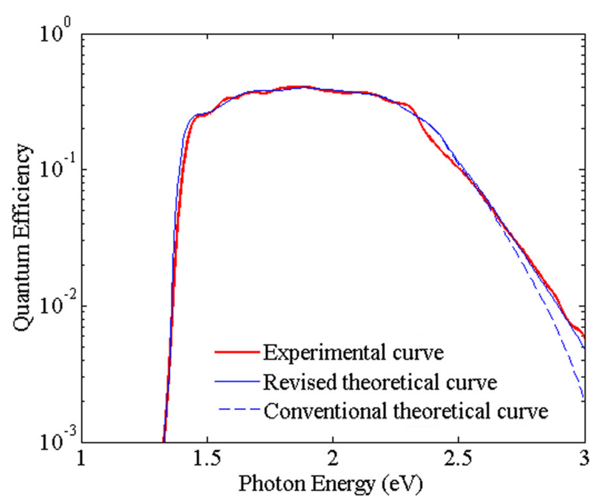

FIG. 6. Experimental quantum efficiency curve of the t-mode $Al_{0.7}Ga_{0.3}As$/GaAs photocathode and the fitted curves via the revised model and the conventional model, respectively.

TABLE I. Fitted performance parameters of the quantum efficiency curves.

Sample type	Electron diffusion length in GaAs layer (μm)	Electron diffusion length in AlGaAs layer (μm)	Back interface recombination velocity (cm/s)	Surface escape probability
r-mode	3.2	1.2	10^7	0.5
t-mode	3.2	1.2	10^5	0.52

Meanwhile, in order to intuitively reflect the effect of the revised quantum efficiency model, we use the revised Eqs. (11) and (12) to fit the experimental curves, respectively, in combination with the conventional Eqs. (13) and (14). As shown in Figs. 5 and 6, for photocathodes operating whether in the r-mode or in the t-mode, it is apparent that the revised quantum efficiency curve can match well with the experimental curve in contrast to the conventional one, especially in the high energy region. Different from the conventional model, the revised quantum efficiency model has taken into account the photoelectrons originating from the AlGaAs buffer layer that absorbs parts of high energy photons. According to the energy gap formula of AlGaAs[20]

$$E_g(x) = 1.424 + 1.594x + x(1-x)(0.127 - 1.310x), \quad (15)$$

where x represents the mole fraction of Al in $Al_xGa_{1-x}As$, the energy gap is calculated to be about 2.2 eV for $Al_{0.6}Ga_{0.4}As$ and 2.4 eV for $Al_{0.7}Ga_{0.3}As$. Consequently, the quantum efficiency in the region above 2.2 eV for the r-mode sample and above 2.4 eV for the t-mode sample should contain the electron contributions from the AlGaAs buffer layer, which is consistent with the experimental results shown in Figs. 5 and 6. The fitted values of the cathode performance parameters through the revised quantum efficiency models are listed in Table I. It is seen from Table I that the r-mode sample has the worse back interface recombination velocity than the t-mode sample. This important performance parameter is related to the cathode material quality itself. As a result of the ultrathin emission layer and the lower electron-reflected potential barrier,[12] the misfit dislocations between the buffer layer and emission layer would increase the electron recombination possibility and reduce the shortwave quantum efficiency. With the aid of the revised models, the cathode performance parameters can be obtained more accurately by a best fit of the experimental quantum efficiency curves. As mentioned above, when the emission layer is very thick or the buffer layer is extremely thin, the effect of buffer layer on quantum efficiency can be neglected.

V. CONCLUSION

In this paper, we have deduced the quantum efficiency models for thin r-mode and t-mode GaAs-based heterojunction photocathodes by considering the photoelectrons generated in the buffer layer. By using the revised models combined with the conventional models, the effects of the thicknesses of emission layer and buffer layer and the back interface recombination velocity on quantum efficiency are analyzed. The results show us the effect of buffer layer on quantum efficiency is closely related to these three factors. Besides, the experimental quantum efficiency curves for thin r-mode and t-mode AlGaAs/GaAs photocathodes are well fitted, which confirms the applicability of the revised model. The revised quantum efficiency models would help to well understand the photoemission mechanism for various thin GaAs-based heterojunction photocathodes.

ACKNOWLEDGMENTS

This work was supported by the National Natural Science Foundation of China (Grant Nos. 61301023, 91433108, and 61261009), and Specialized Research Fund for the Doctoral Program of Higher Education of China (Grant No. 20133219120008).

[1]S. Karkare, D. Dimitrov, W. Schaff, L. Cultrera, A. Bartnik, X. H. Liu, E. Sawyer, T. Esposito, and I. Bazarov, J. Appl. Phys. **113**, 104904 (2013).
[2]K. Aulenbacher, J. Schuler, D. V. Harrach, E. Reichert, J. Röthgen, A. Subashev, V. Tioukine, and Y. Yashin, J. Appl. Phys. **92**, 7536–7543 (2002).
[3]S. Karkare, L. Boulet, L. Cultrera, B. Dunham, X. H. Liu, W. Schaff, and I. Bazarov, Phys. Rev. Lett. **112**, 097601 (2014).
[4]J. P. Estrera, E. J. Bender, A., Giordana, J. W. Glesener, M. Iosue, P. P. Lin, and T. W. Sinor, Proc. SPIE **4128**, 46–53 (2004).
[5]J. W. Schwede, T. Sarmiento, V. K. Narasimhan, S. J. Rosenthal, D. C. Riley, F. Schmitt, I. Bargatin, K. Sahasrabuddhe, R. T. Howe, J. S. Harris, N. A. Melosh, and Z. X. Shen, Nat. Commun. **4**, 1576 (2013).
[6]D. H. Dowell, I. Bazarov, B. Dunham, K. Harkay, C. Hernandez-Garcia, R. Legg, H. Padmore, T. Rao, J. Smedley, and W. Wan, Nucl. Instrum. Methods Phys. Res. A **622**, 685–697 (2010).
[7]C. K. Sinclair, P. A. Adderley, B. M. Dunham, J. C. Hansknecht, P. Hartmann, M. Poelker, J. S. Price, P. M. Rutt, W. J. Schneider, and M. Steigerwald, Phys. Rev. ST Accel. Beams **10**, 023501 (2007).
[8]T. Nakanishi, K. Togawa, T. Baba, F. Furuta, H. Horinaka, T. Kato, Y. Kurihara, H. Matsumoto, T. Matsuyama, T. Nishitani, S. Okumi, T. Omori, T. Saka, C. Suzuki, Y. Takeuchi, K. Wada, K. Wada, and M. Yamamoto, Nucl. Instrum. Methods Phys. Res. A **455**, 109–112 (2000).
[9]W. E. Spicer, Phys. Rev. **112**, 114–122 (1958).
[10]G. A. Antypas, L. W. James, and J. J. Uebbing, J. Appl. Phys. **41**, 2888–2894 (1970).
[11]Y. Z. Liu, J. L. Moll, and W. E. Spicer, Appl. Phys. Lett. **17**, 60–62 (1970).
[12]Y. J. Zhang, J. J. Zou, J. Niu, J. Zhao, and B. K. Chang, J. Appl. Phys. **110**, 063113 (2011).
[13]J. J. Zou and B. K. Chang, Opt. Eng. **45**, 054001 (2006).
[14]S. H. Jung, C. Z. Kim, D. H. Jun, W. Park, H. K. Kang, J. Lee, and H. Kim, Curr. Appl. Phys. **14**, 1476–1480 (2014).
[15]L. B. Jones, S. A. Rozhkov, V. V. Bakin, S. N. Kosolobov, B. L. Militsyn, H. E. Scheibler, S. L. Smith, and A. S. Terekhov, AIP Conf. Proc. **1149**, 1057 (2009).
[16]T. Maruyama, R. Prepost, E. L. Garwin, C. K. Sinclair, B. Dunham, and S. Kalem, Appl. Phys. Lett. **55**, 1686–1688 (1989).
[17]T. Maruyama, E. L. Garwin, R. Prepost, and G. H. Zapalac, Phys. Rev. B. **46**, 4261–4264 (1992).
[18]T. Maruyama, A. Brachmann, J. E. Clendenin, T. Desikan, E. L. Garwin, R. E. Kirby, D.-A. Luh, J. Turner, and R. Prepost, Nucl. Instrum. Methods Phys. Res. A. **492**, 199–211 (2002).
[19]T. Maruyama, E. L. Garwin, R. Prepost, and G. H. Zapalac, Phys. Rev. Lett. **66**, 2376–2379 (1991).
[20]H. C. Casey, D. D. Sell, and K. W. Wecht, J. Appl. Phys. **46**, 250–257 (1975).

[21]D. E. Aspnes, S. M. Kelso, R. A. Logan, and R. Bhat, J. Appl. Phys. **60**, 754–767 (1986).
[22]K. A. Costello, V. W. Aebi, and H. F. Macmillan, Proc. SPIE **1243**, 99–106 (1990).
[23]T. W. Sinor, J. P. Estrera, D. L. Phillips, and M. K. Rector, Proc. SPIE. **2551**, 130–134 (1995).
[24]Y. J. Zhang, J. Niu, J. Zhao, J. J. Zou, B. K. Chang, F. Shi, and H. C. Cheng, J. Appl. Phys. **108**, 093108 (2010).
[25]G. A. Antypas, J. S. Escher, J. Edgecumbe, and R. S. Enck, Jr., J. Appl. Phys. **49**, 4301 (1978).
[26]Y. Sun, Z. Liu, and P. Pianetta, J. Appl. Phys. **102**, 074908 (2007).
[27]S. Moré, S. Tanaka, S. Tanaka, Y. Fujii, and M. Kamada, Surf. Sci. **527**, 41 (2003).
[28]B. J. Stocker, Surf. Sci. **47**, 501 (1975).
[29]Y. J. Zhang, J. Niu, J. J. Zou, B. K. Chang, and Y. J. Xiong, Appl. Opt. **49**, 3935–3940 (2010).